

Unit Cell Design for Space-Fed Surfaces Via Kernel-Based Machine Learning Regression

Original

Unit Cell Design for Space-Fed Surfaces Via Kernel-Based Machine Learning Regression / Beccaria, M.; Soleimani, N.; Trincherò, R.; Pirinoli, P.. - (2025). (2025 URSI International Symposium on Electromagnetic Theory, EMTS 2025 Bologna (Ita) 23-27 June 2025) [10.46620/URSIEMTS25/JDL6926].

Availability:

This version is available at: 11583/3002866 since: 2025-09-08T14:51:38Z

Publisher:

URSI

Published

DOI:10.46620/URSIEMTS25/JDL6926

Terms of use:

This article is made available under terms and conditions as specified in the corresponding bibliographic description in the repository

Publisher copyright

(Article begins on next page)

Unit Cell Design for space-fed antenna via Kernel-based Machine Learning Regression

Michele Beccaria, Nazanin Soleimani, Riccardo Trincherò and Paola Pirinoli

Politecnico di Torino, Torino, Italy; e-mail: {michele.beccaria, nazanin.soleimani, riccardo.trincherò, paola.pirinoli}@polito.it

Abstract

This work explores a novel approach for the automatic design and optimization of unit cells (UCs) via kernel-based machine learning regression. Traditional UC optimization relies on brute-force full-wave simulations, which are computationally expensive and time-consuming. The proposed method uses the Least-Squares Support Vector Machines (LS-SVM) regression to build surrogate models, enabling the efficient design space exploration. The optimal UC geometry obtained by the proposed optimization methodology is then validated through the complete design of a three-layer Transmitarray Antenna (TA), achieving a 32 dB peak gain at 30 GHz with approximately 50% efficiency, a 1-dB bandwidth of 14%, and a 3-dB bandwidth of 28%.

1 Introduction and Motivation

The increasing demand for advanced antenna technologies in evolving scenarios such as 5G/6G, small satellites, SATCOM on the move, automotive radar, and surveillance radar has shifted the focus from traditional microwave frequencies to millimeter-wave bands, often requiring wideband, multi-band, or reconfigurability. Reflectarray (RA) [1]-[3] and Transmitarray (TA) [4]-[7] antennas have emerged as promising solutions, offering planar or flexible designs, cost-effectiveness, ease of fabrication, high efficiency, and precise control over amplitude, phase, and polarization.

At the core of these technologies, including more recent radiating surfaces such as Smart Electromagnetic Skins (SESS) [8], lies the design of the Unit Cell (UC), which is dictated by application-specific technological and electromagnetic requirements. Typically, UC optimization relies on a brute-force approach using full-wave simulations, a process that can take days or even weeks to achieve optimal performance, making the overall design highly inefficient and time-consuming.

In this scenario, Machine Learning (ML) approaches can be seen as promising solutions to reduce the computational cost of the overall optimization task [7, 9, 10, 11]. The underlying idea is to use supervise data-driven ML techniques to build an accurate and fast-to-evaluate surrogate model able to approximate the behavior of a generic EM parametric structure provided by full-wave simulations [7, 10, 13]. The above surrogate model is built via ML regressions (e.g.,

kernel methods, artificial neural networks, etc.) from the results of a “small” set of parametric simulations of the considered EM structure [13, 14]. The obtained surrogate model is available in closed-form, and thus it can be suitably employed within the optimizer iterations [10, 13], as an extremely efficient alternative to the more computationally expensive full-wave simulations.

In this work, the choice to apply the surrogate model to a UC for the design of a Transmitarray Antenna is motivated by the complexity of designing such cells [7]. This complexity arises from the need to manage multiple parameters at the same time (eg. S_{21} and S_{11}) and the critical trade-off between radiation performance and cost. For instance, achieving optimal performance typically requires more than four layers or the introduction of vias, which make the antenna structure more complex and expensive [4]. Specifically, a kernel regression, such as the Least Square Support Vector Machine (LS-SVM) regression [12, 14] is used to build a surrogate model for the S_{21} and S_{11} of the UC element as a function of two geometrical parameters. The models are trained using the results of a set of full-wave simulations. The obtained surrogate models are then used to efficiently optimize the geometry of considered UC to achieve the best radiative performance while keeping the problem complexity low and reducing the antenna cost (e.g., considering only three layers in a TA structure).

2 Proposed Method for Unit Cell design

The Unit Cell proposed here, shown in Fig.1, consists of three identical layers, separated by a spacing $S \simeq \lambda_0/4$. Each layer is composed of a conductive metallic circular ring-shaped slot, deposited on a dielectric substrate of the same shape with a thickness $t = 0.125$ mm, a relative dielectric constant $\epsilon_r = 3$, and losses $\tan \delta = 0.005$. $R_{max} = 2.5$ mm defines the outer radius of the ring gap and is kept constant. R_{min} is the inner radius of the slot, g represents the width of the metallic gap between the ring slot and the surrounding metal, and $p = 5.55$ mm is the periodicity.

The UC has been implemented as an embedded element in a periodic lattice in CST Microwave Studio™, performing a Floquet analysis in the frequency domain. This analysis provides the magnitude and phase response of the transmission coefficient S_{21} , which are used to maximize the transmitted field and compensate for the phase delay of the im-

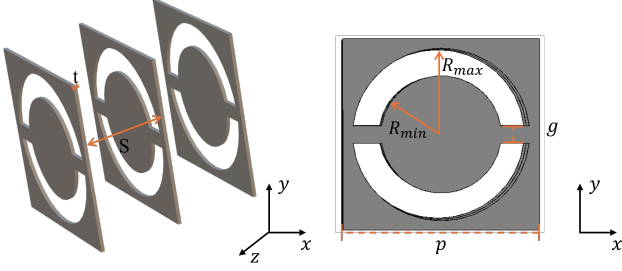


Figure 1. Sketch of the proposed unit cell.

pinging spherical wave on the TA to produce the desired beam pattern. Such compensation is controlled by the geometrical parameter R_{min} that can be varied in an interval of $[0.2, 2]$ mm, while the gap g has to be optimized to minimize the magnitude S_{11} as much as possible, to avoid a low Front-to-back ratio. Its range variation has been chosen to be $[0.2, 0.8]$ mm, due to manufacturing aspects. The complete design has been carried out in the Ka-band at $f_0 = 30$ GHz.

2.1 Surrogate Model

The previously described simulation framework is used to generate the training and test sets required to construct surrogate models that approximate the relationship between the input parameters g and R_{min} and the three outputs of interest, i.e., the magnitude and phase of S_{21} , and the magnitude of S_{11} . To this aim, the considered input parameters are modeled as independent uniform random variables: $g \sim \mathcal{U}(0.2, 0.8)$ mm and $R_{min} \sim \mathcal{U}(0.2, 2)$ mm. A Latin hypercube sampling is applied to generate 300 random samples, which are then used as input to run the corresponding full-wave simulations. The resulting dataset consists of input-output pairs $\{(\mathbf{x}_k, \mathbf{y}_k)\}_{k=1}^{300}$, where $\mathbf{x}_k = [g_k, R_{min,k}]^T$ represents the k -th input configuration, and $\mathbf{y}_k = [\angle S_{21,k}, |S_{21,k}|, |S_{11,k}|]^T$ collects the corresponding outputs.

A subset of 250 randomly selected samples is used as training set $\mathcal{D} = \{(\mathbf{x}_l, \mathbf{y}_l)\}_{l=1}^{L=250}$, while the remaining 50 samples serve as test data to assess the accuracy of the models. The training set \mathcal{D} is then used to train a scalar surrogate model for each of the 3 outputs via the LS-SVM regression [14, 12], which in its dual formulation writes:

$$\tilde{\mathcal{M}}(\mathbf{x}) = \sum_{l=1}^L \beta_l k(\mathbf{x}_l, \mathbf{x}) + b, \quad (1)$$

where β_l are the regression coefficients estimated during the model training, $k(\cdot, \cdot)$ is the kernel function and b is the bias term.

The LS-SVM regression in (1) is used in this work as it provides a non-parametric model with L unknown coefficients $[\beta_1, \dots, \beta_L]^T$, making the surrogate model independent of model complexity and input dimensionality. Its unknowns are efficiently estimated via a convex optimization problem

requiring only the inversion of a square matrix [14, 12], offering advantages in training time and accuracy, particularly when limited training data is available.

A Gaussian RBF kernel function is used within the MATLAB LS-SVMLab Toolbox version 1.8 [15] to train a scalar surrogate model for each output. Specifically, the surrogate models $\tilde{\mathcal{M}}_1$, $\tilde{\mathcal{M}}_2$, and $\tilde{\mathcal{M}}_3$ are trained for $\angle S_{21}$, $|S_{21}|$ in dB, and $|S_{11}|$ in linear scale, respectively.

All three surrogate models achieve high accuracy on the test set, with an R^2 score greater than 0.94. This accuracy is further validated by the parametric plots in Fig. 2, showing the modeled prediction surfaces (gray area) predicted via the surrogate models for $\angle S_{21}$, $|S_{21}|$ (dB) and $|S_{11}|$ (linear scale), as functions of the input parameters g and R_{min} , along with training (black dots) and test (red dots) samples. The results demonstrate the effectiveness of the proposed modeling approach and its reliability for optimization, as most of the training and test data are accurately approximated by the proposed surrogates.

2.2 Unit Cell Optimization

The obtained surrogate models provide an efficient alternative to computational expensive full-wave parametric simulations for optimizing the geometry of the considered UC in Fig. 1. The overall optimization problem is formulated as the search for the optimal parameter g that satisfies the following objectives: (i) maximize the maximum excursion of $\angle S_{21}$, (ii) maximize the average value of $|S_{21}|$, (iii) minimize the average value of $|S_{11}|$, all evaluated over the range of R_{min} within $[0.29, 1.9]$.

After scalarization, the above multi-objective optimization problem is reformulated as a scalar optimization problem:

$$g^* = \underset{g}{\operatorname{argmin}} \underbrace{w_1 f_1(g) + w_2 f_2(g) + w_3 f_3(g)}_{f(g)}, \quad (2)$$

where the normalized cost functions f_1 , f_2 , and f_3 are derived by standardizing their unnormalized counterparts \tilde{f}_1 , \tilde{f}_2 , and \tilde{f}_3 , respectively. These unnormalized functions are computed using the surrogate models as:

$$\tilde{f}_1(g) = \max_{R_{min} \in \mathcal{S}} \{\tilde{\mathcal{M}}_1(g, R_{min})\} - \min_{R_{min} \in \mathcal{S}} \{\tilde{\mathcal{M}}_1(g, R_{min})\} \quad (3)$$

$$\tilde{f}_2(g) = \frac{1}{|\mathcal{S}|} \sum_{R_{min} \in \mathcal{S}} \tilde{\mathcal{M}}_2(g, R_{min}) \quad (4)$$

$$\tilde{f}_3(g) = \frac{1}{|\mathcal{S}|} \sum_{R_{min} \in \mathcal{S}} \tilde{\mathcal{M}}_3(g, R_{min}) \quad (5)$$

where the set $\mathcal{S} = \{R_{min,1}, \dots, R_{min,N}\}$ contains N discrete values of R_{min} uniformly spaced within the considered interval. The weight factors are chosen as $w_1 = 2$, $w_2 = 1$, and $w_3 = -1$ to prioritize the phase excursion while ensuring the minimization of S_{11} .

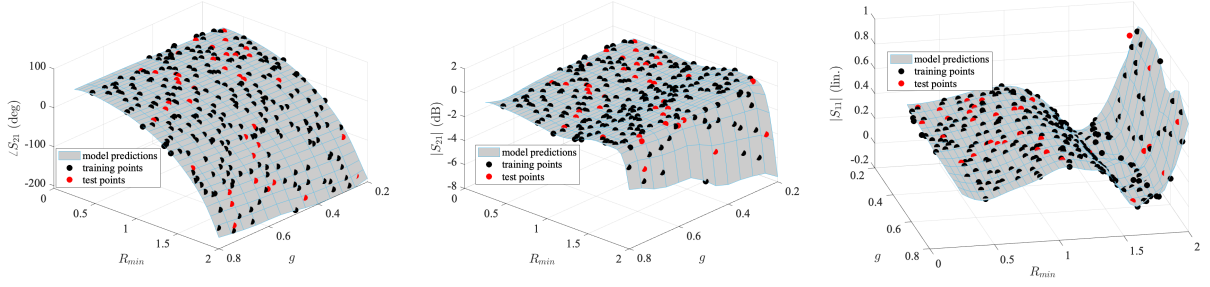


Figure 2. Parametric plots for $\angle S_{21}$, $|S_{21}|$ (dB), and $|S_{11}|$ (linear scale). The surfaces predicted by each surrogate model (gray area) are shown as functions of g and R_{min} , alongside the considered training (black dots) and test (red dots) samples.

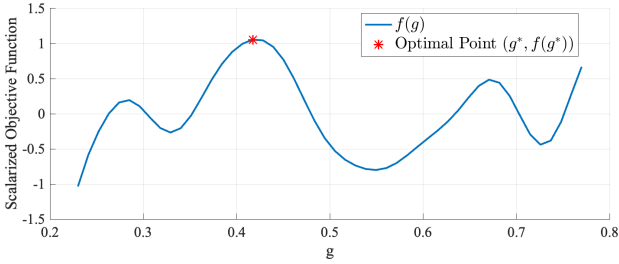


Figure 3. Optimization function $f(g)$ computed over 100 discrete values of g in the interval $[0.23, 0.77]$. The optimal value of the design parameter is $g^* = 0.42$ mm, as determined from the results.

Figure 3 illustrates the overall optimization function $f(g)$, computed over 100 discrete values of g uniformly spaced within the interval $[0.23, 0.77]$. From these results, the optimal value of the design parameter is found to be $g^* = 0.42$ mm.

It is worth noting that the entire optimization process required $50 \times 100 = 5000$ evaluations of the three surrogate models, with a total computational cost of only 84 s. In contrast, a single full-wave simulation for a fixed value of g and R_{min} requires 214 s, meaning that performing 5000 simulations would take approximately 12 days. This highlights the significant efficiency gain achieved through surrogate modeling.

3 Transmitarray Design and Results

The final optimized UC has been assessed through the design of a TA antenna. The considered geometry is sketched in the inset of Fig. 4: the aperture is square, with a side of $D = 16.1\lambda_0$, while the feed is the circular horn introduced in [16], [17], whose radiation pattern can be modeled as a $\cos^{q_f}(\theta)$ function with $q_f = 12.5$ and it is located at a focal distance of $\approx 0.95D$ from the TA surface to achieve an edge taper of -10 dB. The TA is designed to radiate a pencil beam in the broadside direction. It is worth noting that, due to the nature of the UC, comprising only three layers and very thin substrates, the overall antenna structure is highly compact, with a total radiating surface thickness of approximately $0.5\lambda_0$.

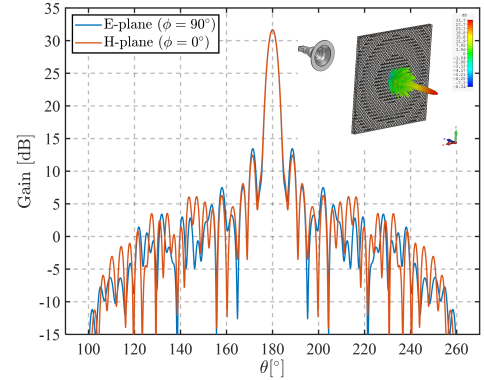


Figure 4. E- and H- planes radiation patterns. Inset: sketch of the Transmitarray layout with its 3D Radiation Pattern at 30 GHz

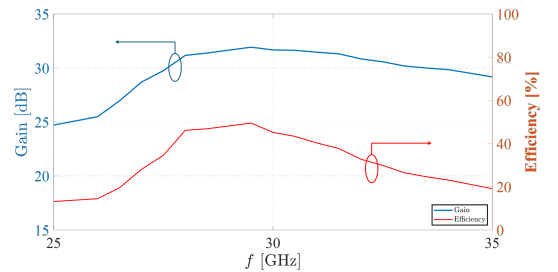


Figure 5. Gain and efficiency variation as a function of frequency.

The numerical analysis of the antenna was performed using a full-wave approach with the Time Domain Solver. Fig. 4 shows the radiation patterns computed at f_0 in the two principal planes. As can be seen, a well-defined pencil beam radiating in the broadside direction is achieved, with low Side Lobe Levels (SLLs) of approximately -20 dB in both principal planes. Moreover, a particularly interesting feature is the behavior of the gain and, consequently, the efficiency as a function of frequency, as shown in Fig. 5. The maximum gain is 32 dB at the central frequency f_0 , leading to an efficiency of approximately 50%. The computed 1-dB bandwidth is found to be 14%, while the 3-dB bandwidth is 28%. These results are very promising, as the optimized unit cell (UC) ensures outstanding radiation performance even though the provided phase range of $\angle S_{21}$ is

limited to approximately 270° . This limitation leads to a distributed phase error along the transmitting surface. This result allows antenna designers to achieve high radiation performance without paying the price of reduced quality when opting for a low-cost structure. In fact, the proposed antenna consists of only three layers, ensuring both simplicity and cost-effectiveness while maintaining excellent performance.

4 Conclusion

This work investigates the performance of a novel approach for the automatic design and optimization of unit cells (UCs) using kernel-based machine learning regression. The proposed optimization method demonstrates significant efficiency gains compared to the computational cost of repeated full-wave simulations. The final UC design was validated through the complete design of a three-layer Transmitarray Antenna, achieving a peak gain of 32 dB at 30 GHz, 50% efficiency, 14% 1-dB bandwidth, and 28% 3-dB bandwidth, confirming its excellent radiation performance.

Acknowledgement

This work was partially supported by the Department of Electronics and Telecommunications (DET), Politecnico di Torino, Turin, in the framework of the project "Next-Gen Smart Electromagnetic Skins via Machine Learning Techniques (NEST)".

References

- [1] J. Huang and J. Encinar, *Reflectarray antennas*. Wiley-IEEE press, 2008.
- [2] A. Niccolai, R. Zich, M. Beccaria and P. Pirinoli, "SNO Based Optimization for Shaped Beam Reflectarray Antennas," *2019 13th European Conference on Antennas and Propagation (EuCAP)*, Krakow, Poland, 2019, pp. 1-4.
- [3] A. Massaccesi *et al.*, "Three-Dimensional-Printed Wideband Perforated Dielectric-Only Reflectarray in Ka-Band," in *IEEE Transactions on Antennas and Propagation*, vol. 71, no. 10, pp. 7848-7859, Oct. 2023.
- [4] A. H. Abdelrahman, F. Yang, and A. Z. Elsherbeni. "Analysis and Design of Transmitarray Antennas." Morgan & Claypool Publishers, 2017.
- [5] M. Beccaria, P. Pirinoli and F. Yang, "Preliminary results on Conformal Transmitarray Antennas," *2018 IEEE International Symposium on Antennas and Propagation & USNC/URSI National Radio Science Meeting*, Boston, MA, USA, 2018, pp. 265-266.
- [6] M. Beccaria, A. Massaccesi, P. Pirinoli and L. H. Manh, "Multibeam Transmitarrays for 5G Antenna Systems," *2018 IEEE Seventh International Conference on Communications and Electronics (ICCE)*, Hue, Vietnam, 2018, pp. 217-221.
- [7] M.A. Belen, et al. "Optimal design of transmitarray antennas via low-cost surrogate modelling," *Sci Rep* 13, 15044, 2023.
- [8] A. Freni, M. Beccaria, A. Mazzinghi, A. Massaccesi, P. Pirinoli, "Low-Profile and Low-Visual Impact Smart Electromagnetic Curved Passive Skins for Enhancing Connectivity in Urban Scenarios," *Electronics*, vol. 12, no. 21, p. 4491, Nov. 2023.
- [9] H. M. Torun and M. Swaminathan, "High-Dimensional Global Optimization Method for High-Frequency Electronic Design," in *IEEE Transactions on Microwave Theory and Techniques*, vol. 67, no. 6, pp. 2128-2142, June 2019, doi: 10.1109/TMTT.2019.2915298.
- [10] W. Na et al., "Advanced EM Optimization Using Adjoint-Sensitivity-Based Multifeature Surrogate for Microwave Filter Design," in *IEEE Microwave and Wireless Technology Letters*, vol. 34, no. 1, pp. 1-4, Jan. 2024, doi: 10.1109/LMWT.2023.3329783.
- [11] J. Zhou et al., "A Trust-Region Parallel Bayesian Optimization Method for Simulation-Driven Antenna Design," in *IEEE Transactions on Antennas and Propagation*, vol. 69, no. 7, pp. 3966-3981, July 2021, doi: 10.1109/TAP.2020.3044393.
- [12] J.A.K. Suykens, et al., *Least Squares Support Vector Machines*, World Scientific Pub Co Inc, 2002.
- [13] N. Soleimani, R. Trincherro and F. Canavero, "Bridging the Gap Between Artificial Neural Networks and Kernel Regressions for Vector-Valued Problems in Microwave Applications," *IEEE Transactions on Microwave Theory and Techniques*, vol. 71, no. 6, pp. 2319-2332, June 2023.
- [14] R. Trincherro, *at al.*, "Machine Learning and Uncertainty Quantification for Surrogate Models of Integrated Devices With a Large Number of Parameters," in *IEEE Access*, vol. 7, pp. 4056-4066, 2019.
- [15] LS-SVMLab, version 1.8; Department of Electrical Engineering (ESAT), Katholieke Universiteit Leuven: Leuven, Belgium, 2011. Available online: <http://www.esat.kuleuven.be/sista/lssvmlab/>.
- [16] M. Beccaria *et al.*, "Feed system optimization for convex conformal reflectarray antennas," *2017 IEEE International Symposium on Antennas and Propagation & USNC/URSI National Radio Science Meeting*, San Diego, CA, USA, 2017, pp. 1187-1188.
- [17] M. Beccaria *et al.*, "Enhanced Efficiency and Reduced Side Lobe Level Convex Conformal Reflectarray," *Applied Sciences*. 2021; 11(21): 9893.